Article ID：1007−7294(2025)06−1000−13

Simulation and Experimental Analysis of Mechanical Properties of a Bidirectional Adjustable Magnetorheological Fluid Damper

YANG Zhi−rong[1], *YE Zhong−min*[1], *LIU Jin−liang*[1], *RAO Zhu−shi*[2], *XIAO Wang−qiang*[3]

(1. School of Marine Engineering, Jimei University, Xiamen 361021, China; 2. State Key Laboratory of Mechanical System and Vibration, Shanghai Jiao Tong University, Shanghai 200240, China; 3. School of Aerospace Engineering, Xiamen University, Xiamen 361102, China)

Abstract: The aim of this study is to address the issues associated with traditional magnetorheological fluid (MRF) dampers, such as insufficient damping force after power failure and susceptibility to settlement. In order to achieve this, a bidirectional adjustable MRF damper was designed and developed. Magnetic field simulation analysis was conducted on the damper, along with simulation analysis on its dynamic characteristics. The dynamic characteristics were ultimately validated through experimental testing on the material testing machine, thereby corroborating the theoretical simulation results. Concurrently, this process generated valuable test data for subsequent implementation of the semi-active vibration control system. The simulation and test results demonstrate that the integrated permanent magnet effectively accomplishes bidirectional regulation. The magnetic induction intensity of the damping channel is 0.2 T in the absence of current, increases to 0.5 T when a maximum forward current of 4 A is applied, and becomes 0 T when a maximum reverse current of 3.8 A is applied. When the excitation amplitude is 8 mm and the frequency is 2 Hz, with the applied currents varying, the maximum damping force reaches 8 kN, while the minimum damping force measures at 511 N. Additionally, at zero current, the damping force stands at 2 kN, which aligns closely with simulation results. The present paper can serve as a valuable reference for the design and research of semi-active MRF dampers.

Key words: magnetorheological fluid (MRF); damper; permanent magnet; finite element analysis; test of mechanical properties

CLC number: U664.21 **Document code:** A **doi:** 10.3969/j.issn.1007−7294.2025.06.013

0 Introduction

The magnetorheological fluids (MRFs), an integral component of MR materials, exhibit the remarkable attribute of reversible control over their rheological properties, thereby rendering them extensively investigated and applied. MRF primarily consists of liquid and soft magnetic particles exhibiting high magnetic conductivity. The addition of active additives is frequently employed to ensure the stability of

Received date：2024−12−21

Foundation item：Supported by the National Natural Science Foundation of China (52475104); Guiding Project of Science and Technology Plan of Fujian Province (2024H0015) and Leading Innovation Project of China National Nuclear Group (22GFC-JJ12-475)

Biography：YANG Zhi-rong(1981−), male, associate professor, M. Sc. supervisor, E-mail: yzhirong2000@126.com.

MRF[1]. The application of a magnetic field enables MRF to undergo rapid and reversible phase transition from liquid to semi-solid, thereby offering the advantages of swift response time and reversibility. A MRF damper is an application device of MRF that offers the advantages of continuous adjustable damping force, rapid response speed, high output capacity, and a simple structure. It has extensive use in semi-active vibration control. The primary operational modes of the system include valve type, extrusion flow type, shear type, and shear valve type. The shear mode offers a lower damping force and is seldom employed. Due to the limitations of its operational mode, the extrusion type is commonly employed in such applications as brakes and clutches, whereas the shear valve type combining the advantages of both shear and valve types with a simplified structure makes it extensively utilized[2]. Wang et al[3] developed a novel MRF damper for mining applications. This damper incorporates a shear valve structure and is subjected to two-dimensional modeling using ANSYS software. Subsequently, the two-dimensional and three-dimensional magnetic induction intensities were obtained through simulation analysis. Li[4] designed a labyrinth-type double-channel valve MRF damper. He simulated the magnetic field line and got the cloud map of magnetic induction intensity distribution using ANSYS software. Zhang[5] designed a suspension curved magnetic circuit MRF damper. By strategically arranging the internal structure of the damper, the magnetic field lines traverse the damping channel multiple times, thereby enhancing the efficiency of magnetic field utilization. The magnetic circuit simulation of the damper employs Maxwell magnetic analysis software to acquire the distribution of magnetic field lines and magnetic induction intensity.

Stanway et al[6] proposed an idealized mechanical model, namely Bingham model, which is a mathematical representation characterizing the dynamic behavior of a specific fluid and finds extensive application in describing non-Newtonian fluids such as MRF. Based on this premise, Gamoto et al[7] proposed an enhanced Bingham model by incorporating a linear structure to establish a Bingham visco-elastic-plastic model. The findings demonstrated the model's capability in accurately forecasting the dynamic response of MRF dampers. Subsequently, Wang et al[8] enhanced the model by employing the piecewise fitting function method and incorporating the inverse tangent function model, based on their investigation of mechanical properties of various complex MRF dampers. The improved Bingham model was compared with actual test output values, demonstrating a significant enhancement in accuracy. Yi et al[9] proposed a Bouc-Wen model consisting of a set of parallel damping elements and elastic elements. The H-B model proposed by Zhang et al[10] utilizes a combination of neural network and least square method for parameter identification, enabling accurate calculation of the damping force of MRF dampers based on the obtained relationship between parameters and current. In order to accurately depict the relationship between nonlinear damping force and velocity, numerous researchers have conducted further investigations into the dynamics model of MRF dampers, encompassing models such as the nonlinear viscous double viscosity model[11], Sigmoid model[12], double Sigmmoid model[13], and modified Dahl model[14]. The establishment of these models enhances the simulation techniques for characterizing the mechanical properties of dampers.

In order to address the issues commonly found in traditional MRF dampers, such as insufficient damping force following power failure and susceptibility to settlement, this paper presents the design and development of a bidirectional adjustable MRF damper. Even in the event of a failure in the external power supply system, the damper still maintains a certain damping output value owing to the presence of permanent magnets. The magnetic field simulation analysis was conducted as the first step, followed by the simulation and analysis of dynamic characteristics. Finally, the theoretical simulation results were validated through testing on a material testing machine, providing test data for subsequent semi-active vibration control systems.

1 Structural design and development of a bidirectional adjustable MRF damper prototype

1.1 Structural design and operational principle

To address the limitations of traditional MRF dampers, such as insufficient output force at zero current and incomplete demagnetization in inverter-type dampers, a novel MRF damper design is proposed based on bidirectional adjustment using permanent magnets. The fundamental structure of the damper is illustrated in Fig. 1. It adopts a shear valve-type double-rod configuration, comprising components such as Shafts A and B, outer cylinder, left end cover, left positioning disk, Stepped Magnetic Conductive Ring I, permanent magnet, Stepped Magnetic Conductive Ring II, right positioning disk, right end cover, auxiliary cylinder, screw, excitation coil, and straight cylindrical magnetic conductive ring. Notably, the permanent magnet and energized excitation coil together form a composite magnetic circuit. At zero current, the permanent magnet alone generates the magnetic field, producing a moderate output force in the damping gap through optimized design. By applying maximum forward and reverse currents to the excitation coil, the magnetic induction intensity within the gap can be accordingly enhanced and weakened, resulting in maximum and minimum output forces. This study refers to this method of controlling the output force of the MRF damper by adjusting the direction of current in the excitation coil as bidirectional damping force modulation.

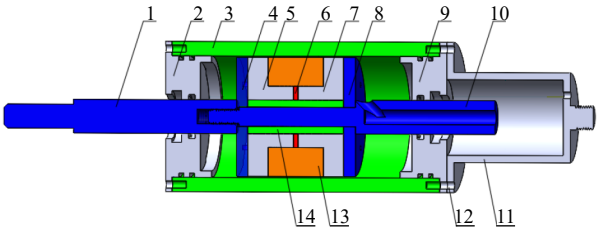

1. Shaft B 2. Left end cover 3. External cylinder block 4. Left positioning disc 5. Step Type Magnetic Ring Ⅰ 6. Permanent magnet 7. Step type magnetic guide ring Ⅱ 8. Right positioning disc 9. Right end cover 10. Shaft A 11. Auxiliary cylinder 12. Screw 13. Excitation coil 14. Straight cylinder type magnetic guide ring

Fig.1 Structure diagram of bidirectional adjustable MRF damper

As illustrated in Fig. 2, when a forward current is applied, the magnetic potential of the permanent magnet and the magnetic potential generated by the excitation coil produce a co-directional magnetic field within the damping channel. Consequently, under the influence of the magnetizing field produced by the magnetic potential of the excitation coil, the operating point of the permanent magnet shifts upward along the demagnetization curve, leading to a gradual increase in the magnetic flux density at the damping channel until the MRF fluid reaches magnetic saturation. At this point, the damper achieves its maximum output force. Conversely, when a reverse current is applied, the magnetic potentials of the permanent magnet and the excitation coil generate an opposing magnetic field within the damping channel. As a result, under the effect of the demagnetizing field produced by the magnetic potential of the excitation coil, the operating point of the permanent magnet moves downward along the demagnetization curve, causing the magnetic flux density at the damping channel to gradually

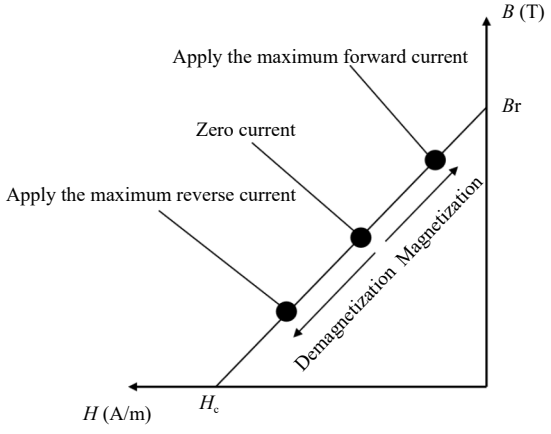

Fig.2 Diagram of operating point motion of permanent magnet

decrease until it reaches zero. The residual magnetic flux of the permanent magnet circulates only between the permanent magnet and the magnetic conduction channel. At this juncture, the damper attains its minimum output force. Neodymium-iron-boron type permanent magnets exhibit an ideal linear demagnetization characteristic, with the hysteresis loop at any point on the demagnetization curve essentially coinciding with the demagnetization curve. These magnets do not experience permanent demagnetization under external magnetic fields, making them suitable for the MRF damper described herein.

1.2 Structural parameters and prototype

Fig. 3 illustrates the detailed structural dimensions of the bidirectional adjustable MRF damper. In accordance with vibration mitigation requirements, the maximum output force of the designed damper is 8 kN, with a dynamic adjustment coefficient of 13. The iron core and cylinder are fabricated from pure iron DT4, while the MRF utilized is of the MRF-350 type. A performance comparison between this type of MRF and Lord Company's MRF-132DJ is presented in Tab. 1. Leveraging the aforementioned material properties and damper specifications, the key structural dimension parameters were determined using a simplified design methodology, as outlined in Tab. 2. Fig. 4 depicts the principle prototype of the bidirectional adjustable MRF damper after processing and assembly.

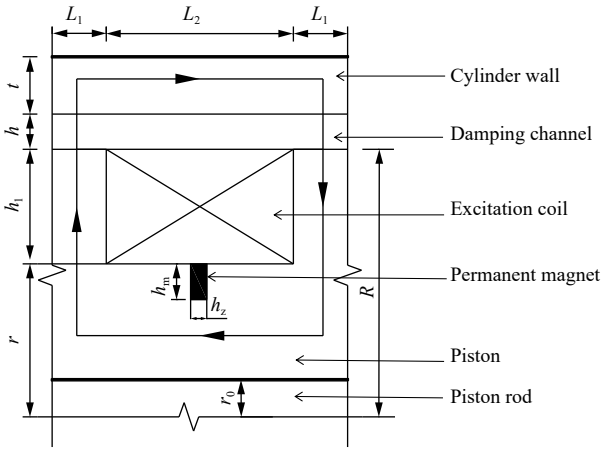

Fig.3 Schematic diagram of the structural dimensions of the bidirectional adjustable MRF damper

Fig.4 Principle prototype of bidirectional adjustable MRF damper

Tab.1 Performance comparison between MRF-350 and MRF-132DJ

Items	MRF-350	Lord's MRF-132DJ
Density/(g·cm^{-3})	2.98–3.10	2.98–3.18
Zero field viscosity/(mPa·s)	350–450 (γ=1000 s^{-1}, 40 ℃)	100 (800 s^{-1}, 40 ℃)
Shear stress/kPa	> 70	40–100
Resistance to settlement	Standing at room temperature for 3 months, the settlement ratio is less than 10%, and it is easy to disperse evenly	The long-term static settlement is less than 20%, and the settlement is soft and non-hardening
Applicable temperature/(℃)	−30–130	−40–130

Tab.2 Key structural dimension parameters of the bidirectional adjustable MRF damper

r/mm	h/mm	r_0/mm	h_1/mm	L_1/mm	L_2/mm	t/mm	h_z/mm	N	h_m/mm
13	0.8	4	12	8.5	24	6	2	180	6

2 Magnetic field simulation and analysis of MRF damper

The finite element model of the MRF damper with bidirectional regulation has been developed utilizing ANSYS Maxwell, a large-scale general-purpose commercial finite element magnetic field analysis software. The two-dimensional cross-section structure of the right half of the piston simulation model is used to simplify the damper piston, considering its axisymmetric nature. The model can be divided into four distinct regions, as illustrated in Fig. 5. The red region represents the magnetic isolation area, while the green region corresponds to the permeability zone. Additionally, the orange region denotes the excitation coil area, and the purple region signifies the MRF zone.

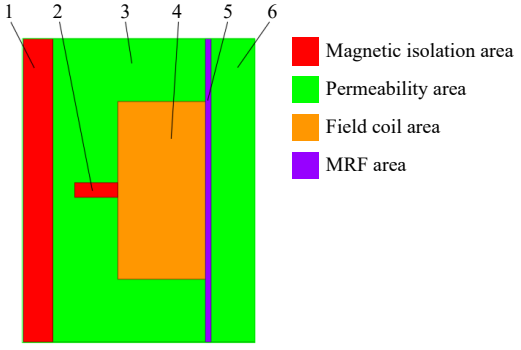

1. Piston rod 2. Permanent magnet 3. Iron core 4. Excitation coil 5. MRF 6. Outer cylinder body

Fig.5 Two-dimensional model diagram

Three sets of simulation schemes are established. The first set involves the excitation coil not applying current, with the magnetic field solely generated by the permanent magnet. The second set involves aligning the direction of the magnetic field generated by the current in the excitation coil with that of the permanent magnet. The third set involves applying current to the excitation coil to produce a magnetic field opposite to that of the permanent magnet. The distribution diagram of magnetic field lines, magnetic induction intensity, and magnetic vectors in the internal section of the damper piston are represented by Fig. 6, Fig. 7, and Fig. 8 respectively under three different conditions: no current in the excitation coil, maximum forward current applied by the excitation coil, and maximum reverse current applied by the excitation coil.

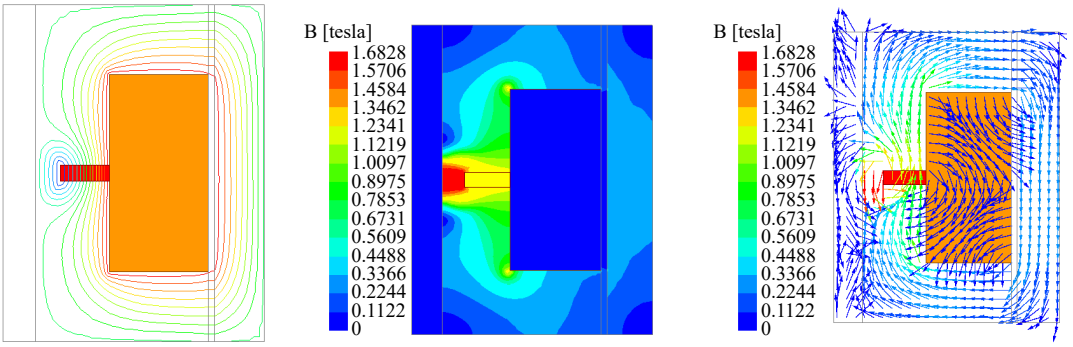

（a）Distribution of magnetic field lines

（b）Cloud map of magnetic induction intensity distribution

（c）Vector diagram illustrating the distribution of magnetic induction intensity

Fig.6 Analysis results of the magnetic field in the absence of current application

As depicted in Fig. 6, even when the coil is not energized, the magnetic field lines still traverse through both the piston and MRF of the damping channel, thereby forming a closed loop. The presence of permanent magnet ensures the maintenance of a specific magnetic field strength within the piston, resulting in an average magnetic induction intensity of approximately 0.2 T at the damping channel. The magnetic field lines generated by permanent magnet exhibit a clockwise orientation. Fig. 7 illustrates that when a maximum forward current of 4 A is applied to the coils, the magnetic field lines in the damping channel become denser. Under the combined influence of the magnetic field generated by the permanent magnet and that generated by

the coils, there is a significant enhancement in the average magnetic induction intensity at the damping channel, reaching approximately 0.5 T. The magnetic vector distribution inside the damper piston exhibits a higher degree of orderliness compared to the magnetic vector distribution generated solely by the permanent magnet. The observation from Fig. 8 reveals that when a maximum reverse current of 3.8 A is applied to the coils, there is an absence of magnetic field lines in the damping channel. The average magnetic induction intensity in the damping channel is approximately 0 T.

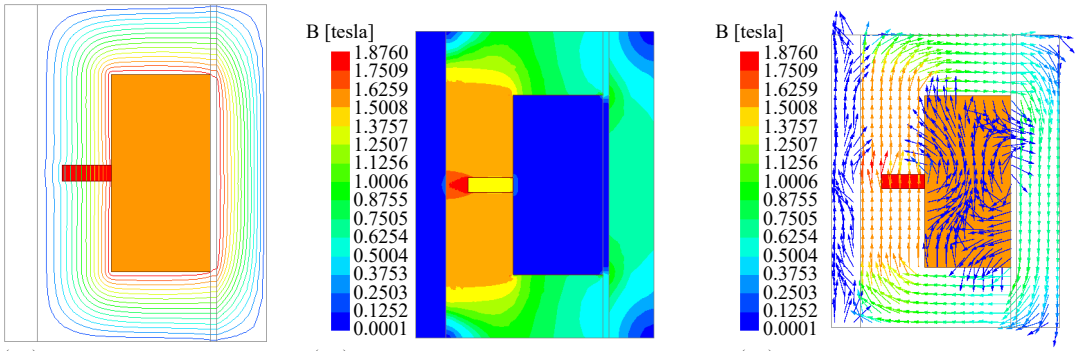

（a）Distribution of magnetic field lines　（b）Cloud map of magnetic induction intensity distribution　（c）Vector diagram illustrating the distribution of magnetic induction intensity

Fig.7 Analysis results of the magnetic field under the maximum forward current application

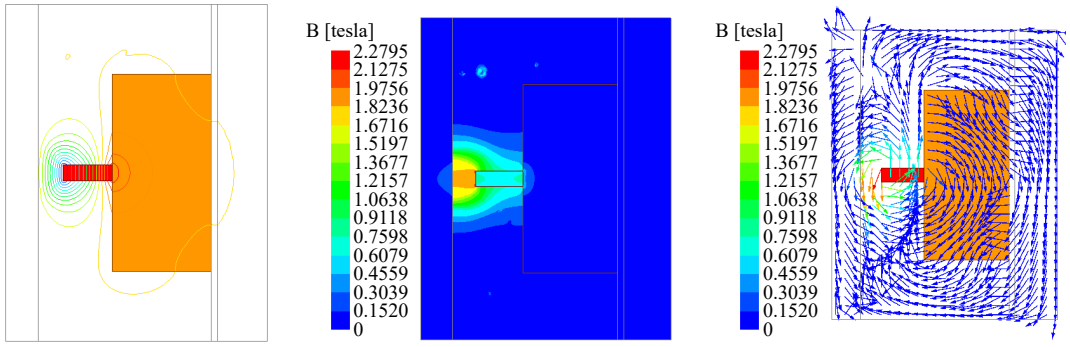

（a）Distribution of magnetic field lines　（b）Cloud map of magnetic induction intensity distribution　（c）Vector diagram illustrating the distribution of magnetic induction intensity

Fig.8 Analysis results of the magnetic field under maximum reverse current application

3 Simulation and analysis of dynamics characteristics of MRF dampers

The dynamics characteristics of a MRF damper were simulated and analyzed using Matlab software in order to investigate the influence of various parameters on its mechanical properties. This was done based on the damping force mechanical model, as well as the relationship between shear yield stress of MRF and magnetic induction intensity, which was obtained through Maxwell 2D magnetic field simulation software. The Bingham plate working model suggests that the damping force in shear valve type can be approximated as the damping force in valve mode, which comprises uncontrollable viscous damping force and controllable Coulomb damping force. The former is directly proportional to velocity, while the latter can be considered as a frictional force and is dependent on the direction of piston movement and yield stress. The displacement of the damper piston is denoted as x, and the damping force formula is established as follows:

$$F=\frac{12\eta LA_{\mathrm{p}}{}^{2}}{\pi D'h^{3}}\dot{x}+\frac{3LA_{\mathrm{p}}}{h}\tau_{y}\mathrm{sgn}(\dot{x})=C\dot{x}+C_{1}\tau_{y}\mathrm{sgn}(\dot{x}) \tag{1}$$

The relevant damper parameters were substituted into the above formula, yielding values of 6644.7 for parameter C and 0.1154 for parameter C_1.

The relationship between the current I passing through the excitation coil and the magnetic induction intensity B can be determined through simulation results of the magnetic field. Here, I represents the current passing through the excitation coil, while B denotes the magnetic induction intensity at the damping channel. The resulting curve depicting this relationship is illustrated in Fig. 9.

The curve can be considered as a piecewise function curve. It is divided into three segments at I=0.4 A and I=1.1 A, and the component segment functions are determined through polynomial fitting for each of the three segments respectively. The correlation between magnetic induction intensity B and input current I in the damping channel is as follows:

$$B=\begin{cases}0.0446I+0.1718,\ -3.8\leqslant I<0.4\\ -0.7767I^{3}+1.637I^{2}-0.7386I+0.2717,\ 0.4\leqslant I<1.1\\ -0.002\,907I^{3}+0.016\,67I^{2}+0.010\,74I+0.3801,\ 1.1\leqslant I\leqslant 4\end{cases} \tag{2}$$

The MRF-350, discussed in this paper, exhibits a dynamic viscosity η of 0.8 Pa·s. Fig. 10 illustrates the relationship between shear yield strength τ_y and magnetic induction strength B. It can be achieved through polynomial fitting as outlined below:

$$\tau_{y}=-33\,640\cos(5.733B)-8769\sin(5.733B)+37\,980 \tag{3}$$

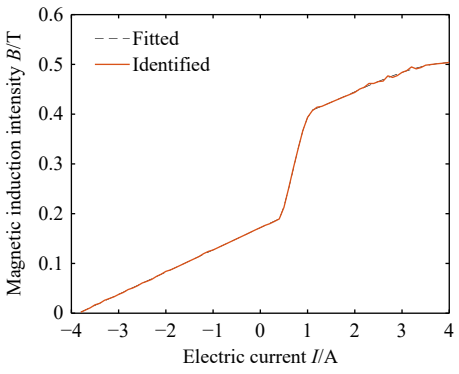

Fig.9 Fitting curve of magnetic induction intensity B and electric current I

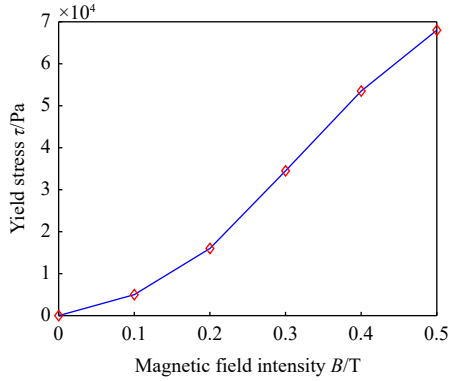

Fig.10 Relationship between yield stress and magnetic field intensity of MRF-350

The dynamic simulation model of the damping force of the MRF damper was established based on Eq. (1) to investigate its working performance. By utilizing the Simulink module in Matlab software, the relationship between damping force and piston displacement and velocity under various excitation current, frequency, and amplitude was calculated.

The damping force, displacement, and velocity curves are depicted in Fig. 11 for a sinusoidal excitation with an amplitude of 8 mm and frequency of 2 Hz. The current passing through the excitation coil is varied as −3.8 A, 0 A, 1 A, 2 A, and 4 A respectively. The increase in current passing through the coil, as depicted in Fig. 11(a), leads to a proportional augmentation of its damping force. When a maximum current of 4 A is applied to the coil, the damper exhibits its highest damping force, reaching approximately 8 kN. Conversely, when a maximum reverse current of 3.8 A passes through the coil, the minimum value of the damping force is around 500 N, representing viscous damping. The correlation between the damping force exerted by the damper and the velocity of the piston is illustrated in Fig. 11(b). The velocity curve of the damping force

exhibits a reverse 'Z' shape, as illustrated in the figure. The viscous damping force of the damper, as indicated by Eq. (1), is directly proportional to the velocity of the piston. As the piston speed increases, so does the viscous damping force; however, its contribution to the overall damping force remains relatively small. Consequently, with an increase in velocity, there is only a marginal increment in the damping force.

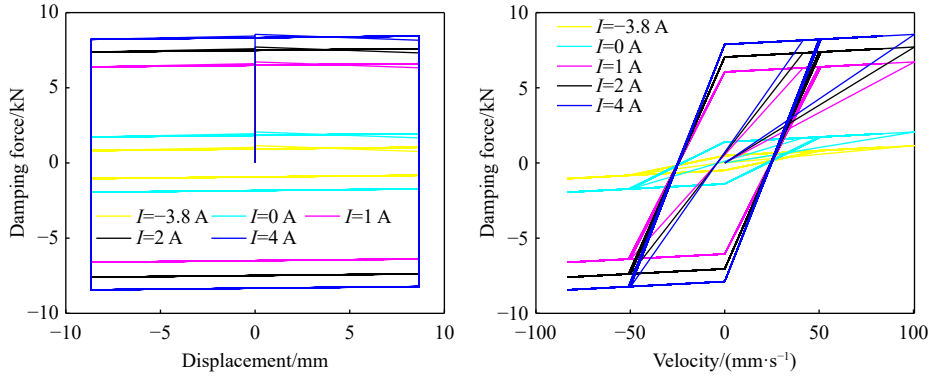

（a）Damping force-displacement curve　（b）Damping force-velocity curve

Fig.11 Relationship between damping force, displacement and velocity under various current conditions

The damping force, displacement, and velocity curves are again depicted in Fig. 12 under various frequencies with sinusoidal excitation amplitude of 8 mm and loading current of 1 A. The external excitation frequencies considered are 0.5 Hz, 1 Hz, 2 Hz, 3 Hz and 4 Hz. The figure illustrates that as the excitation frequency increases, there is only a slight increase in the total damping force. This can be attributed to the fact that changes in excitation frequency primarily affect piston speed when acting on the MRF damper. On the other hand, Coulomb damping force is determined by input current in the excitation coil and various structural parameters, remaining unaffected by piston movement speed. The viscous damping force is influenced by the piston speed; however, due to its relatively small contribution to the overall damping force, variations in external excitation frequency have a minimal impact on the damping force.

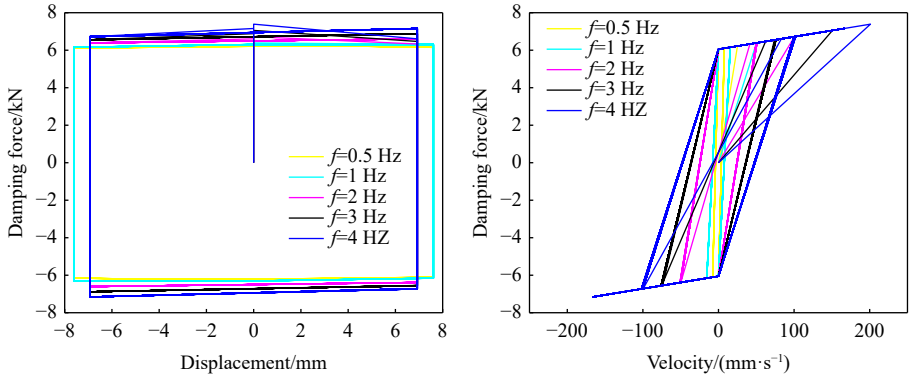

（a）Damping force-displacement curve　（b）Damping force-velocity curve

Fig.12 Relationship between damping force, displacement and velocity under various frequencies

The damping force, displacement, and velocity curves are also depicted in Fig. 13 with sinusoidal excitation frequency of 2 Hz, loading current of 1 A, while varying external excitation amplitudes of 4 mm, 6 mm, 8 mm, 10 mm, and 12 mm. The curve reveals that the variation in damping force resulting from changes in external excitation amplitude is negligible, indicating that altering the amplitude of external excitation is tantamount to modifying the piston head displacement. The motion speed of the MRF damper piston is jointly determined by the amplitude and frequency of external excitation. When the frequency

remains constant, an increase in the amplitude of external excitation results in a higher motion speed of the piston. Consequently, there is also an increase in the corresponding viscous damping force. However, since the viscous damping force has a minimal impact on the total damping force, changes in external excitation amplitude have little effect on overall damping force.

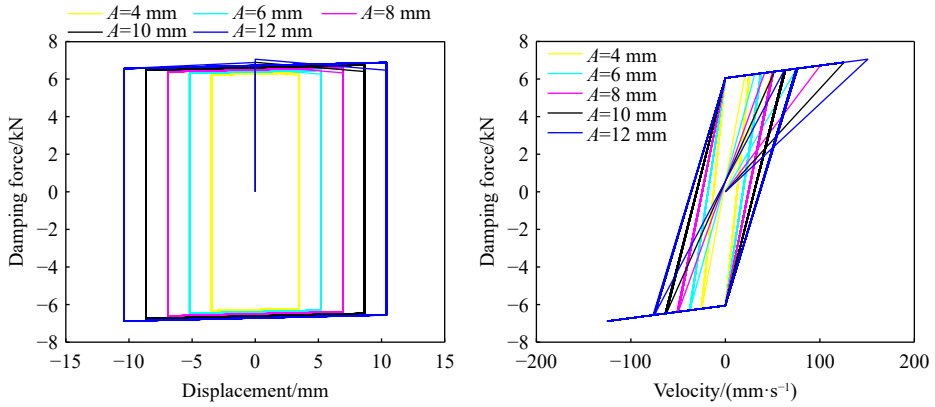

（a）Damping force-displacement curve （b）Damping force-velocity curve

Fig.13 Relationship between damping force, displacement and velocity under various amplitudes

4 Test of mechanical properties of MRF damper

The accuracy of the theoretical simulation is further verified, and test data for the subsequent semi-active control system is provided by constructing a damper mechanical performance test system and analyzing its dynamic performance. The mechanical property test system of MRF damper is illustrated in Fig. 14. The model of the material testing machine is KCH-701-20, with a frequency range of 0.01 Hz to 300 Hz, a maximum displacement range of −25 mm to +25 mm, a maximum acceleration of 30*g*, a maximum speed of 50 cm/s, and a dynamic loading force range of −20 kN to +20 kN. The test system primarily comprises six components, namely the experimental loading terminal, MRF damper, electro-hydraulic servo controller, servo hydraulic oil source, DC power supply, and computer for signal processing and analysis.

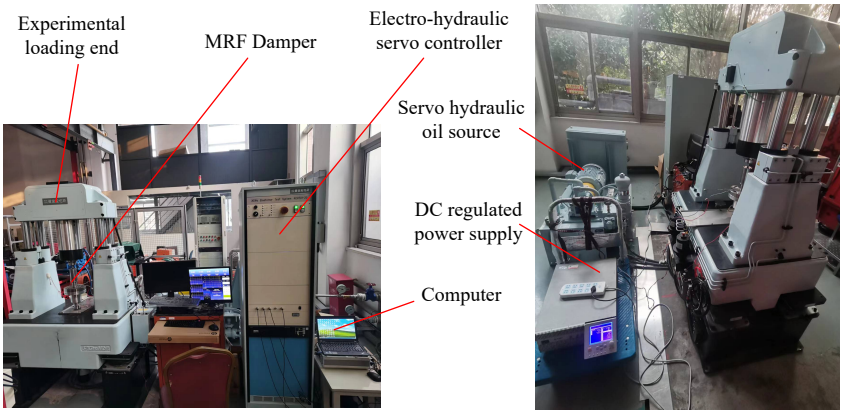

Fig.14 Mechanical properties test system of MRF damper

The effects of different variables on the mechanical properties of dampers are discussed in the following three cases: (1) constant amplitude and frequency with varying current, (2) constant amplitude and current with varying frequency, and (3) constant current and frequency with varying amplitude.

4.1 Correlation between damping force, displacement and velocity under various current conditions

The excitation amplitude and frequency remain constant, while the dynamic performance of the damper is evaluated through variations in input current. With the amplitude set to 8 mm and the frequency to 2 Hz, currents of −3.8 A, 0 A, 1 A, 2 A, and 3 A is applied into the excitation coil, respectively. The relationship between damping force, displacement and velocity at various current levels is illustrated in Fig. 15.

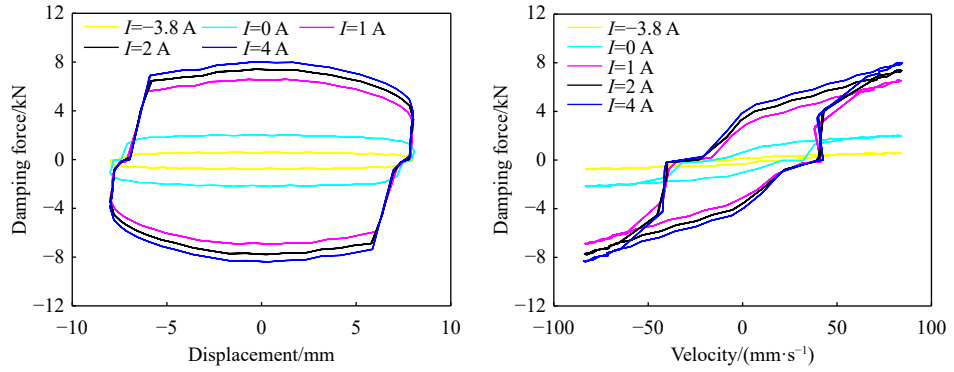

（a）Damping force-displacement curve　（b）Damping force-velocity curve

Fig.15 Correlation between damping force and displacement, velocity under various current conditions

The figure illustrates that the damping force generated by the MRF damper increases proportionally with the current increment. The increase in yield stress of the MRF due to the magnetic field generated by passing current through the excitation coil leads to an enhanced damping force. As depicted in the figure, at 0 A, the damper's output damping force is 2 kN. At −3.8 A, a minimum output damping force of 511.49 N is observed. When the input current reaches 4 A, the damping force achieves its maximum value of 8 kN.

4.2 Correlation between damping force, displacement and velocity at various frequencies

The excitation amplitude and the input current are set to a fixed value, and the impact of changes in excitation frequency on the output damping force of the damper is investigated. The amplitude should be set to 8 mm, the input current to 1 A, and the frequency successively adjusted to 0.5 Hz, 1 Hz, 2 Hz, 3 Hz, and finally 4 Hz. The relationship between damping force, displacement, and velocity at various frequencies is illustrated in Fig. 16.

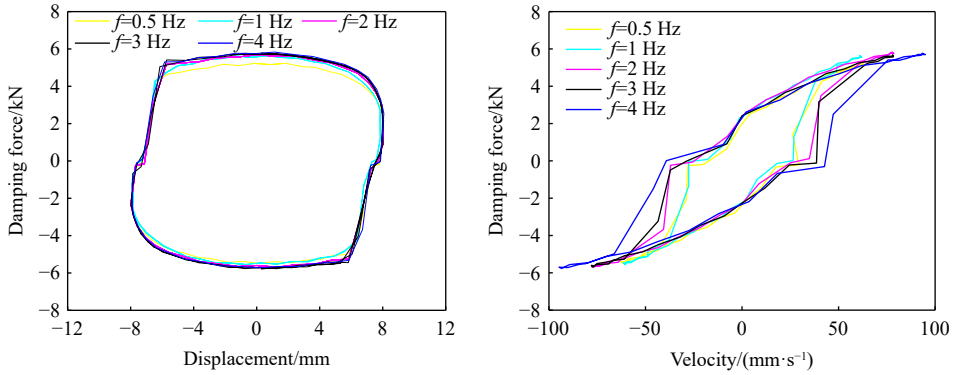

（a）Damping force-displacement curve　（b）Damping force-velocity curve

Fig.16 Correlation between damping force, displacement and velocity at various frequencies

The figure illustrates that the output damping force of the damper remains relatively stable when there is a change in excitation frequency, and the maximum output damping force remains consistent at different frequencies. The above analysis reveals that the output damping force is influenced by both viscous damping

and Coulomb damping. However, it should be noted that the frequency increase has no impact on the Coulomb damping force, but only results in a slight augmentation of the viscous damping force. As a result, there is only a marginal alteration in the output damping force at each frequency.

4.3 Correlation between damping force, displacement and velocity under varying amplitudes

The relationship between the damping force, displacement and velocity of the damper under different excitation amplitudes is illustrated in Fig. 17, with the excitation frequency and input current kept constant. The excitation frequency is set to 2 Hz, the input current is set to 1 A, and the excitation amplitude is set to 4 mm, 6 mm, 8 mm, 10 mm, and 12 mm respectively.

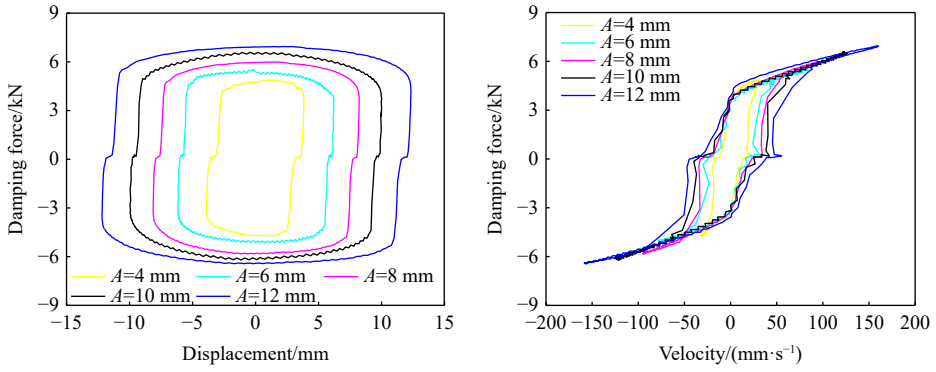

（a）Damping force-displacement curve （b）Damping force-velocity curve

Fig.17 Correlation between damping force, displacement and velocity under varying amplitudes

The figure illustrates that as the excitation amplitude increases, the maximum output damping force also exhibits a corresponding increase while maintaining constant frequency and current. The reason for this is that, when the frequency remains constant, an increase in amplitude results in a higher motion speed of the piston. Consequently, the increased piston speed leads to an augmented viscous damping force, while the change in speed does not affect the Coulomb damping force. Therefore, as the excitation amplitude increases, there is a slight upward trend observed in the total output damping force of the damper.

5 Conclusions

The present study focuses on the design and development of a bidirectional adjustable MRF damper utilizing permanent magnet technology. Firstly, a simulation and analysis of the magnetic field of the damper is conducted. Subsequently, the damper's dynamic characteristics are simulated and analyzed. Finally, experimental tests are performed on a material test machine to validate the theoretical simulation results. The main conclusions can be summarized as follows:

(1) This MRF damper can effectively achieve bidirectional regulation of damping force. When subjected to the maximum reverse current, it can be completely demagnetized. The magnetic field distribution within the damping channel under three operational states satisfies the design specifications.

(2) The damper reaches the medium, maximum, and minimum output states under conditions of zero current, maximum forward current, and maximum reverse current, respectively. It exhibits a relatively high dynamic regulation coefficient, thereby effectively realizing the design concept of bidirectional damping force regulation.

(3) The output force of the damper in the zero-current state lies within the range defined by its maximum

and minimum output forces. This characteristic not only ensures the fail-safe performance of the damper in the event of a power failure but also effectively mitigates the settlement phenomenon associated with MRF.

References

[1] Ju B X. Lü B. Structural design and magnetic circuit analysis of integrated electromagnetic piston with MR Damper[J]. Journal of Magnetic Materials and Devices, 2022, 53(2): 39–45.

[2] Li Z X, Xu L H. New MR damper and semi-active control design theory[M]. Beijing: Science Press, 2012: 1–25.

[3] Wang X, Chen F, Li A, et al. Research on the performance of a novel MR damper for mining[J]. Journal of Vibration Engineering & Technologies, 2023, 11: 3947–3958.

[4] Li Y. Design and experimental study of a labyrinth type double-channel valve MR damper[D]. Liuzhou: Guangxi University of Science and Technology, 2023.

[5] Zhang C Q. Design and optimization of a MR damper for suspension curved magnetic circuit[D]. Nanjing: Nanjing Forestry University, 2023.

[6] Stanway R, Sproston J L, Stevens N G. Non-linear identification of an electrorhelological vibration damper[J]. IFAC Identification and System Parameter Estimation, 1985, 16(10): 195–200.

[7] Gamoto D R, Filisko F E. Dynamic mechanical studies of electrorheological materials: Moderate frequencies[J]. Rheology, 1991, 35(3): 399.

[8] Wang Q, Ma J C, Zhu Y R, et al. Bingham mechanical model improvement and parameter identification of MR damper[J]. Mechanical Design & Manufacture, 2024(1): 10–13+19.

[9] Yi F, Dyke S J, Caicedo J M, et al. Experimental verification of multiinput seismic control strategies for smart dampers[J]. Engineering Mechanics, 2001, 127(11): 1152–1164.

[10] Zhang Z K, Zhang H, Yan Y Y. Parameter identification method of H-B model of MR damper based on least square method and BP neural network[J]. Machine Tool & Hydraulics, 2024, 52(4): 126–131.

[11] Choi Y T, Bitman L, Wereley N M. Nondimensional analysis of electrorheological dampers using an Eyring constitutive relationship[J]. Journal of Intelligent Material Systems & Structures, 2005, 16(5): 383–394.

[12] Hu G L, Liu Q J, Li G, et al. Simulation and analysis of Sigmoid mechanical model of adjustable MR damper[J]. Machine Tool & Hydraulics, 2016, 44(24): 9–15.

[13] Li X L, Li H N. Double sigmoid model and experimental verification of Mr Dampers[J]. Journal of Vibration Engineering, 2006, 19(2): 168–172.

[14] Miao Z, Long H Y, Li Y G, et al. Establishment and simulation verification of Dahl model modified by MR damper[J]. Mechanical Engineering & Automation, 2018, 12(1): 88–90.

双向调节磁流变阻尼器的力学特性仿真及试验分析

杨志荣[1], 叶忠民[1], 柳金良[1], 饶柱石[2], 肖望强[3]

（1. 集美大学 轮机工程学院 福建 厦门 361021; 2. 上海交通大学 机械系统与振动全国重点实验室, 上海 200240; 3. 厦门大学 航空航天学院, 福建 厦门 361102）

摘要: 针对传统磁流变阻尼器的断电后阻尼力过小以及易沉降等问题, 本文设计并研制一种双向调节磁流变阻尼器, 对其进行磁场仿真分析, 并对其动力学特性进行仿真分析, 最后在试验机上对其动力学特性进行试验测试, 验证理论仿真结果, 同时为后续的半主动振动控制系统提供试验数据。仿真和试验结果表明: 该阻尼器内置永磁体可以达到双向调节的目的, 其阻尼通道处在不施加电流时的磁感应强度为 0.2 T, 施加正向最大电流 4 A 时的磁感应强度为 0.5 T, 施加反向最大电流 3.8 A 时磁感应强度为 0 T; 当激励幅值为 8 mm, 频率为 2 Hz, 施加不同电流时, 试验测试其最大阻尼力为 8 kN、最小阻尼力为 511 N、零电流下的阻尼力为 2 kN, 与仿真结果相近。本文可为相关的半主动磁流变阻尼器设计及研究提供参考。

关键词: 磁流变液; 阻尼器; 永磁体; 有限元分析; 力学性能测试

中图分类号: U664.21 **文献标识码:** A

基金项目: 国家自然科学基金面上项目（52475104）; 福建省科技计划引导性项目（2024H0015）; 中核集团领创科研项目（22GFC-JJ12-475）

作者简介: 杨志荣（1981–）, 男, 博士, 集美大学副教授。